Analysis and Optimization of Polarization-Insensitive Semiconductor Optical Amplifiers with Delta-Strained Quantum Wells

Yong-Sang Cho, *Member, IEEE*, and Woo-Young Choi

***Abstract*—Polarization sensitivity of semiconductor optical amplifiers (SOAs) with delta-strained quantum-well (QW) structures is investigated. The valence band structures and TE, TM optical gain spectra are calculated for the various delta-strained QW structures. It is shown that the number and location of the delta layers affect the polarization dependence of the delta-strained quantum well SOA signal gains. The optimal delta-strained QW structure for the SOA application is identified and its theoretical verification is provided.**

***Index Terms*—Delta-strain, optical amplifiers, optical gain, polarization-sensitivity, quantum well, semiconductor.**

I. Introduction

RECENTLY, there has been a growing interest in the semiconductor optical amplifier (SOA) for optical switching and signal processing applications because of its integratability with other optical devices and large nonlinearity. The optical nonlineariy in the SOA is used in realizing optical 3R regeneration (reamplifying–reshaping–retiming) [1] wavelength switching matrix in wavelength division mulitplexing (WDM) systems [2] and wavelength converters using cross gain or phase modulation [3] or four-wave mixing [4]. In these applications, dependence of the SOA gain on polarization is one of the major performance-limiting factors. The polarization sensitivity of the quantum well (QW) SOA stems from the different quantization levels for heavy-hole (HH) bands, which provide the TE-mode dominant optical gain, and light-hole (LH) bands, which provide the TM-mode dominant optical gain. In addition, the difference in the confinement factors for TE and TM modes in the SOA waveguide contribute to the different TE and TM signal gains.

One method for eliminating the SOA polarization sensitivity is to use the bulk active layer with the square-shaped cross section [5]. But such an SOA has a very small waveguide width, which results in a large coupling loss when the SOA is coupled to optical fiber. In order to avoid this problem, a mode converter can be used [6], but this complicates the SOA fabrication process. Although it is possible to use the low tensile-strained bulk active layer to make the waveguide width sufficiently large [7], it is preferred for many applications to use the QW SOA which has larger nonlinearity than the bulk SOA [8]. In order to realize a polarization-insensitive QW SOA, several different QW structures have been used: low tensile-strained QWs [9], [10], QWs with tensile barriers [11], tensile-strained QWs with compressive barriers [12], alternation of tensile and compressive QWs [13]–[16], and the delta-strained QW, in which the strain is applied only at a shallow and highly strained layer, called the delta layer [17]–[19]. Among these, it is reported that the delta-strained QW can yield a polarization-insensitive SOA at 1550 nm [18].

Carlo *et al.* performed theoretical analysis of the delta-strained QW using the tight-bonding method [17], but their study was limited to a particular type of delta-strained QW in which one delta layer is located at the center of the QW. In this paper, various delta-strained QW structures are analyzed in which the number and the position of the delta layers are systematically varied. From our analysis, the optimal delta-strained QW structure for SOA application is identified and theoretical verification is provided.

II. Structure and Modeling of Delta-Strained QW SOA

The delta-strained QW structure investigated in this paper consisted of one InGaAs/InGaAsP QW in which 3-monolayer-thick (about 9 Å) pseudomorpic GaAs delta layers are embedded. It is assumed that all the layers are epitaxially grown on the InP substrate. The lattice mismatch between InP and GaAs is -3.8%. The delta-strained well is surrounded by 1.3 μm-InGaAsP quaternary layers, which also act as the SCH layer. The total well thickness is adjusted so that the optical gain peaks at around 1550 nm.

Fig. 1(a)–(c) show the valence band energy diagrams for three types of delta-strained QWs that are investigated in this paper. In Type I, one delta layer is inserted; in Type II, two delta layers; and in Type III, three delta layers. SOAs based on Type I [18] and Type III [19] have been experimentally demonstrated, and a waveguide modulator based on Type II has been demonstrated [20]. The polarization dependence of SOAs based on these three types of delta-strained QWs is systematically investigated in this paper. As can be seen from the figure, HH and LH bands are separated at the delta layer due to the strain. In the figure, thick lines are used for HH bands and thin lines for LH bands. d_1, d_2, and d_3 in the figure represent the distance between the delta layer

Manuscript received August 28, 2000; revised November 27, 2000. This work was supported in part by Advanced Photonics Technology Project in Korea and also by the Brain Korea 21 Project.

The authors are with the Department of Electrical and Electronic Engineering, Yonsei University, Seoul, Korea.

Publisher Item Identifier S 0018-9197(01)02327-2.

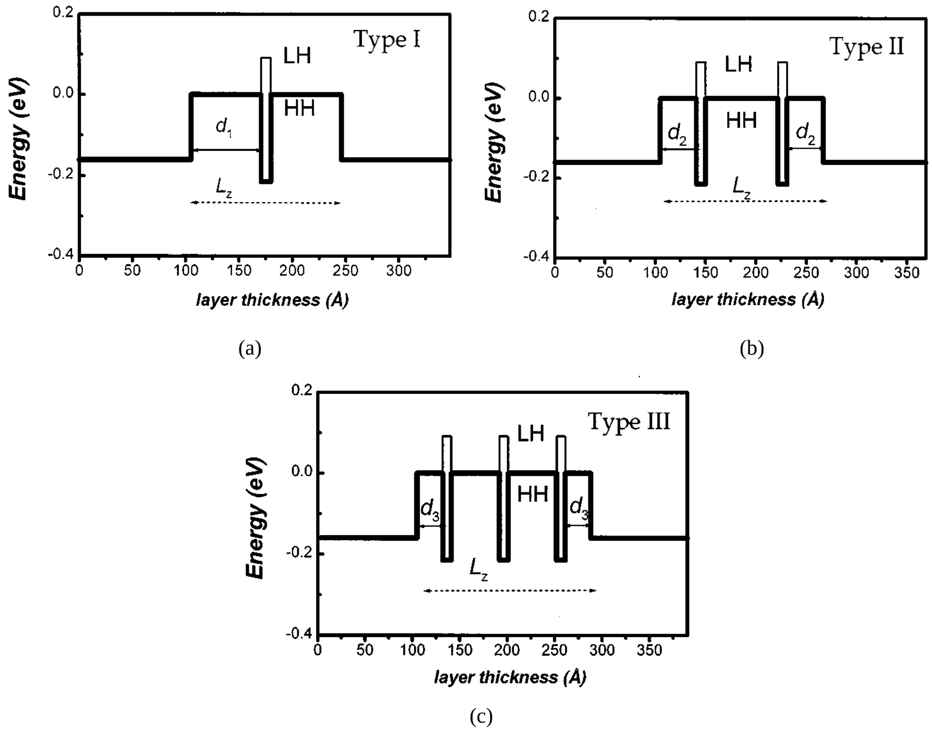

Fig. 1. Valence band energy diagrams for: (a) Type I; (b) Type II; and (c) Type III structures. Thin lines are LH bands and thick lines are the HH bands.

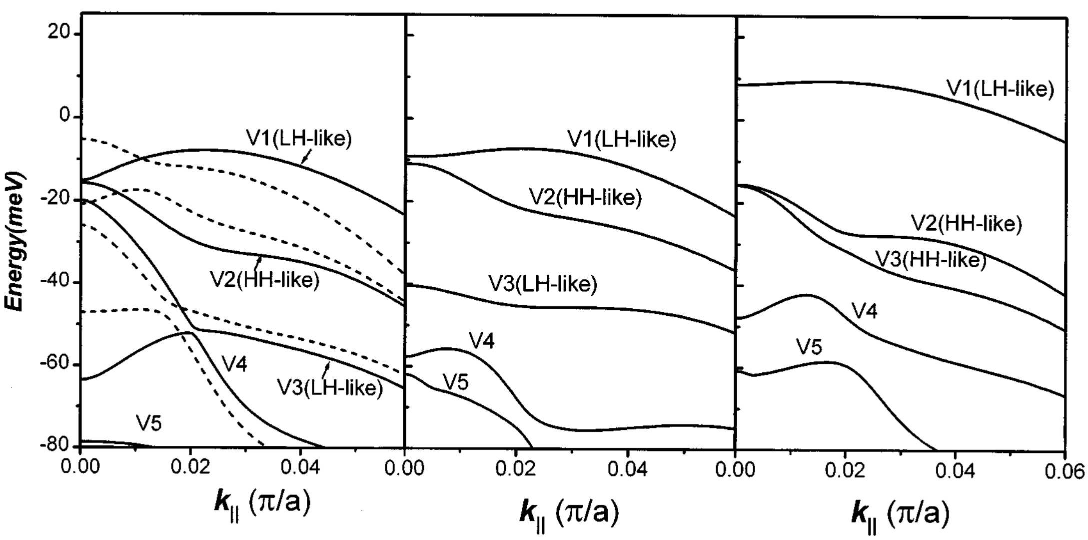

Fig. 2. $E - k$ diagrams for: (a) Type I (solid lines) and unstrained QW (dashed lines); (b) Type II; and (c) Type III structures.

and the InGaAsP SCH layer for each type of delta-strained QW. The changes in the SOA polarization-sensitivity as functions of these parameters are investigated.

The band offsets for conduction and valence bands are obtained from the model-solid theory [21]. For valence band analysis, a 4×4 Luttinger–Kohn Hamiltonian based on the $k \cdot p$ method is used with the strain effect consideration. The effective mass equations are solved by the finite element method (FEM), which has a faster conversion time and is more efficient for complicated structures than the finite difference method (FDM) [22]. The efficiency provided by the FEM allows us to compare many different delta-strained QW structures without any difficulty in computation time. Material parameters used in the calculation are obtained from [23]. The optical gain calculation is done with the density matrix formalism [24]. It is assumed that the equal numbers of electrons and holes exist in the QW. For many body effects, only the bandgap renormalization effect is considered because the Coulomb enhancement of the optical gain is negligible in the case of tensile-strained QWs [25]. The amount of bandgap shrinkage due to renormalization is obtained from the empirical equation given in [26].

Polarization-dependent optical confinement factors for the SOA waveguide structure are calculated by solving the 1-D waveguide problem for TE and TM polarizations [27]. The waveguide structure used in the calculation has 0.216-μm-thick SCH layers and infinitely long InP claddings. The ratios between the calculated TM and TE confinement factors for Type I, II, and III structures are 0.6568, 0.6559, and 0.6553, respectively.

The SOA TE and TM signal gains that are used for evaluating the SOA polarization-sensitivity are defined as follows [28]:

$$G_{\mathrm{TE,\,TM}} = 10L[\Gamma_{\mathrm{TE,\,TM}}\, g(\omega)_{\mathrm{TE,\,TM}} - \alpha_i]\log_{10}(e), \quad \text{[dB]} \tag{1}$$

where

- Γ optical confinement factor;
- $g(w)$ optical gain;
- L SOA length;
- α_i loss in the SOA.

For our analysis, $L = 1$ mm and $\alpha_i = 5\ \mathrm{cm}^{-1}$ are used, and the SOA facet reflectivity is assumed to be zero.

III. Polarization-Sensitivity of Delta-Strained QW SOA

In QWs without delta layers, HH band energy levels are usually higher than those of LH bands, resulting in more TE gain than for the TM case. In delta-strained QWs, as shown in Fig. 1, the delta layer introduces larger valence band discontinuity for HH bands than LH bands, and the quantized energy levels for HH bands experience a larger shift downward than those for the LH bands that shift upward. This is clearly demonstrated by Fig. 2(a), where the valence band E–k relations are shown for a Type I structure with the delta layer in the middle of the QW (solid lines) and also for a QW without any delta layers (dotted lines). Since each valence subband has HH and LH characteristics for $k_{\|} > 0$ due to the band mixing effect, it is necessary to estimate the strength of TE and TM transitions for the subband of interest in order to identify it as HH- or LH-like. Fig. 3 shows calculated transition strength for several transitions possible with the delta-strained QW whose band structure is shown in Fig. 2(a). From these, we can determine that the top valence subband is LH-like as the TM transition strength for the transition between the first conduction subband (c1) and the top valence subband (v1) is much larger than the TE transition strength. Consequently, it can be determined that the delta layer pushes up the LH band and pushes down the HH band so much that their order is reversed. In Fig. 2, the top three valence subbands are identified as LH- or HH-like from the transition strength calculations. It should be noted that our results shown in Figs. 2(a) and 3 that are obtained from the FEM-based effective mass approximation agree very well with the results obtained from much more elaborate, but more time-consuming, tight binding analysis [17].

The influence of the delta layer location on the TE, TM gain is shown in Fig. 4 in which the TE and TM optical gain spectra for a Type I structure are shown for several values of d_1. The injected carrier density of $45 \times 10^{18}\ \mathrm{cm}^{-3}$ is used for this calculation. As d_1 is increased, i.e., the delta layer moves toward the well center, the peak TE gain is reduced while the peak TM gain is increased. In order to determine the optimal location for the delta layer, we have to consider the SOA signal gain rather than the optical gain, since there exists a difference in the TE, TM waveguide confinement factors. Fig. 5 shows the spectra of the SOA polarization-sensitivity (ΔG) defined as the difference in the TM and TE signal gains ($G_{\mathrm{TM}} - G_{\mathrm{TE}}$) at several values

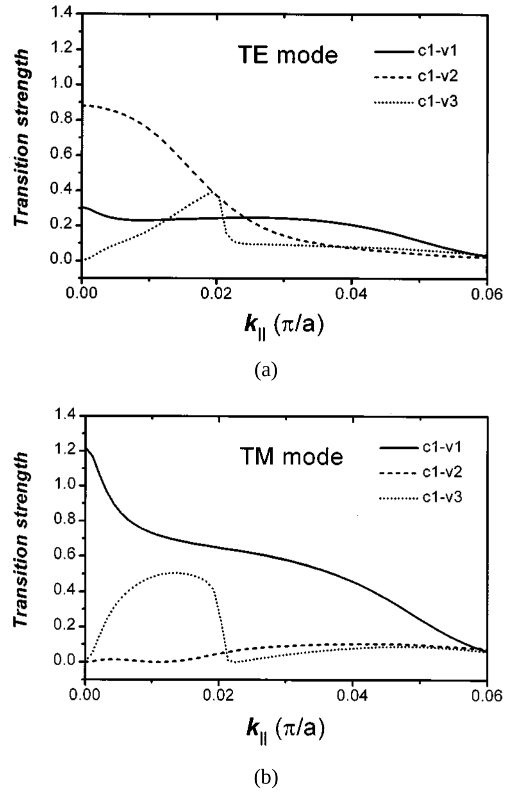

Fig. 3. Relative transition strength for: (a) TE and (b) TM polarization for Type I structure.

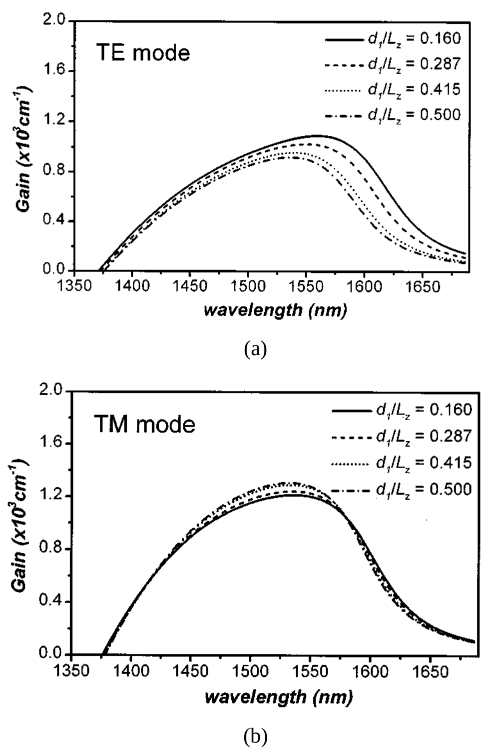

Fig. 4. Gain spectra for Type I structure at various delta layer locations for: (a) TE and (b) TM mode.

of d for each type of the delta-strained SOA structure. From this, the optimal delta layer location can be determined for each type. For Type I, as shown in Fig. 5(a), the ΔG spectrum moves up as d_1 is increased, and the optimal location for the delta layer

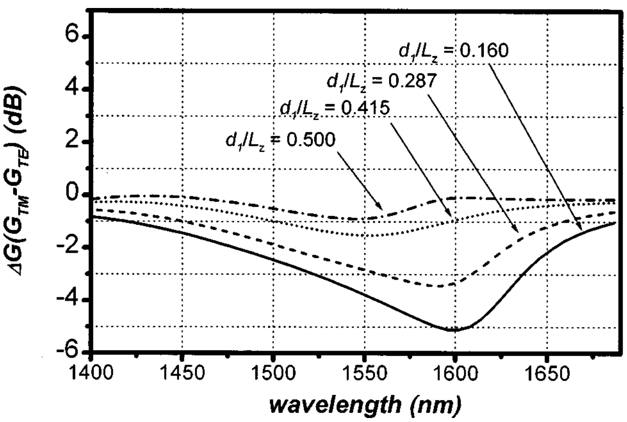

(a)

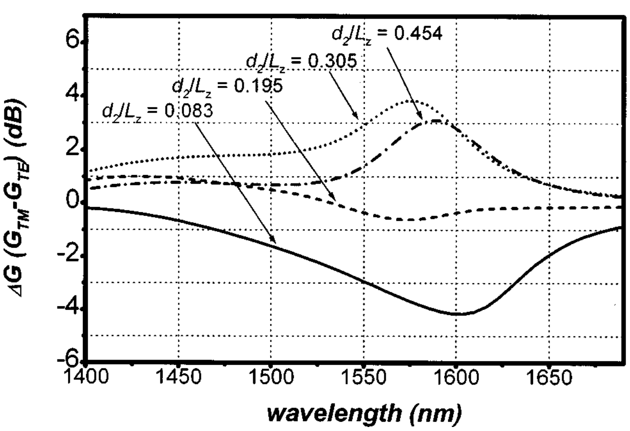

(b)

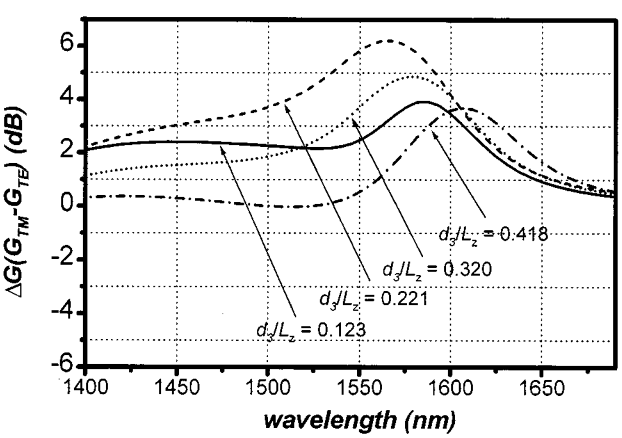

(c)

Fig. 5. Difference in SOA signal gains ($G_{\rm TM} - G_{\rm TE}$) at various delta layer locations for: (a) Type I; (b) Type II; and (c) Type III structures.

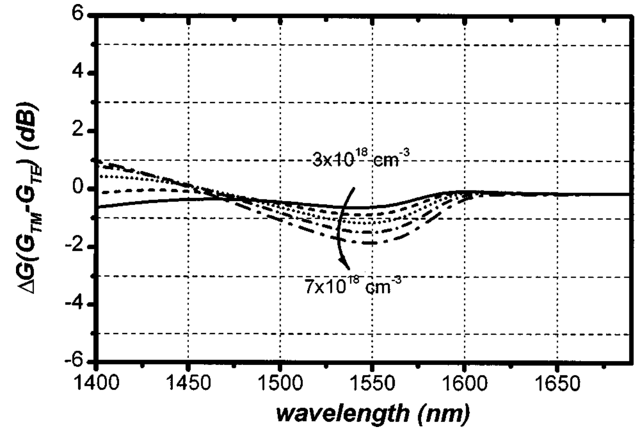

(a)

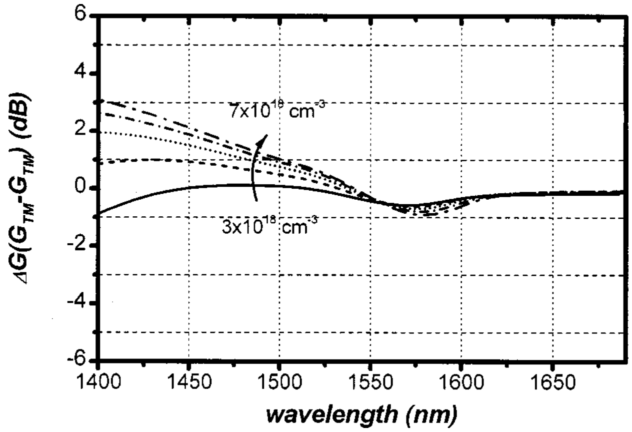

(b)

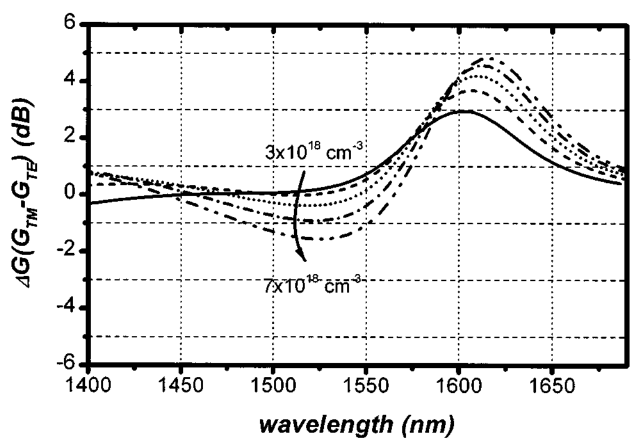

(c)

Fig. 6. Difference in SOA signal gains ($G_{\rm TM} - G_{\rm TE}$) at various injected carrier densities for the delta-strained QWs with the optimal delta layer locations: (a) Type I; (b) Type II; and (c) Type III structures. Carrier density is increased in the step of 1×10^{18} cm^{-3}.

is the well center. Fig. 4 shows that the TM gain is larger than that for TE at this optimal location, and this is needed in order to offset the difference in the confinement factors. For Type II, ΔG gets larger as d_2 gets larger but it comes down when d_2 is sufficiently large. This can be understood as the influence of the change in the amount of perturbation that the odd-mode envelope functions experience that are located away from the well center. For Type III, a similar trend is observed. The optimal location of the delta layer can be determined as $d_1/L_z = 0.5$ for Type I, $d_2/L_z = 0.195$ for Type 2, and $d_3/L_z = 0.418$ for Type III.

For many SOA applications, SOA polarization-insensitivity should be maintained for a wide range of injected carrier densities. We investigated the dependence of polarization-sensitivity on the injected carrier density for each type of delta-strained QW with the optimal delta layer location. The injected carrier density investigated ranges from 3 to 75×10^{18} cm^{-3}. As seen in Fig. 6, each type shows a different dependence on the injected carrier densities. If we limit the wavelength range of interest to around 1550 nm, Type II shows the least dependence. This can be understood from the valence band structures shown in Fig. 2, where the valence band structures of three types of optimized delta-strained QWs are shown. All three structures have the LH-like top subband, which ensures the larger TM gain needed to offset a larger TE confinement factor. The difference lies in the amounts of separation between the first and second, and second and third subbands. It can be observed that Type-II structure has a distinctive feature in that the first two subbands are closely placed for the wide ranges of $k_{||}$, and the third subband is far away from the first two. As the injected carriers increase, the range of valence band energies involved in the transition increases. This does not cause much change in the polarization sensitivity in Type II, as closely placed first top subbands maintain the ratio of the TE and TM contribution over a wide range of $k_{||}$ without interference from the third subband which would enhance the TM contribution. Consequently, an SOA based on the Type-II structure has a signal gain at around 1550 nm, which is least dependent on the injected carrier densities.

A similar observation has been made for a waveguide modulator with delta-strained QWs, each of which has two delta layers with $d_2/L_z = 0.227$. The polarization sensitivity was maintained within 3 dB for the reverse bias range of 0–2.5 V over the wavelength range of 1600–1630 nm [20]. We can also observe that transitions for wavelengths shorter than 1550 nm in Type II have a strong dependence on the injected carrier densities. as such transitions have to involve the third valence subband due to their transition energies. In addition, it can be observed that the Type-III structure, with its second and third subbands closely located to eachother, has the largest dependence on injected carrier densities. We believe that the Type-II QW structure that has been identified as the optimal delta-strained QW structure can be realized without too much difficulty in the manner similar to that used for realizing various types of delta-strained QWs [18]–[20].

IV. Conclusion

The valence band structures and optical gains of three types of delta-strained InGaAs/InGaAsP QWs and the polarization-dependent signal gains of SOAs based on such QWs are investigated in this paper. In our analysis, the location of the delta layers was varied so that the optimal delta layer location could be identified. In addition, the polarization dependence of the SOA signals gains was investigated as a function of the SOA injected carrier densities. It was found that the Type-II structure with two delta layers located at $d_2/L_z = 0.195$ is the optimal structure for SOA applications. The reason for this is that this QW structure has a band structure in which the top valence subband is LH-like, a second subband which is HH-like and tracts the first subband, and the third subband is far away from the first two.

Although our analysis is based on a particular set of numerical parameters which may not always be applicable for real applications, the ease with which our analysis was performed with the simple effective mass approximation will allow us to analyze and optimize any delta-strained QW that may have different parameters. In addition, the key observation made for the optimal structure should be valid for any QW structure to be used for polarization-insensitive SOA applications.

References

[1] K. S. Jepsen, A. Buxens, A. T. Clausen, H. N. Poulsen, B. Mikkelsen, and K. E. Stubkjaer, "All-optical network interface for bit synchronization and regeneration," *Electron. Lett.*, vol. 34, 1998.

[2] E. Almstrom, C. Popp Larsen, L. Gillner, W. H. van Berlo, M. Gustavsson, and E. Berglind, "Experimental and analytical evaluation of packaged 4×4 InGaAsP/InP semiconductor optical amplifier gate switch matrices for optical networks," *J. Lightwave Technol.*, vol. 14, pp. 996–1004, 1996.

[3] T. Durhuus, B. Mikkelsen, C. Joergensen, S. Lykke Danielsen, and K. E. Stubkjaer, "All-optical wavelength conversion by semiconductor optical amplifiers," *IEEE J. Quantum Electron.*, vol. 14, pp. 942–954, 1996.

[4] L. Y. Lin, J. M. Wiesenfeld, J. S. Perino, and A. H. Gnauck, "Polarization-insensitive wavelength conversion up to 10 Gb/s based on four-wave mixing in a semiconductor optical amplifiers," *IEEE Photon. Technol. Lett.*, vol. 10, pp. 955–957, 1998.

[5] P. Doussier, P. Garabedian, C. Graver, D. Bonnevie, T. Filion, E. Derouin, M. Mannot, J. G. Provost, D. Leclerc, and M. Klenk, "1.55-μm polarization-independent semiconductor optical amplifier with 25 dB fiber to fiber gain," *IEEE Photon. Technol. Lett.*, vol. 6, pp. 170–172, 1994.

[6] N. Yoshimoto, K. Magari, T. Ito, Y. Kawaguchi, K. Kishi, Y. Kondo, Y. Kadota, O. Mitomi, Y. Yoshikuni, Y. Hasumi, Y. Tohmori, and O. Nakajima, "Spot-size converted polarization-insensitive SOA gate with a vertical tapered submicrometer stripe structure," *IEEE Photon. Technol. Lett.*, vol. 10, pp. 510–512, Apr. 1998.

[7] J.-Y. Emery, T. Ducellier, M. Bachmaon, P. Doussiere, F. Pommereau, R. Ngo, F. Gaborit, L. Goldstein, G. Laube, and J. Barrau, "High performance 1.55-μm polarization insensitive semiconductor optical amplifier based on low-tensile-strained bulk GaInAsP," *Electron. Lett.*, vol. 33, pp. 1083–1084, 1997.

[8] J. Yao, G.-H. Duan, and P. Gallion, "Strong signal analysis of optical nonlinearity in single-quantum-well and double-heterostructure lasers," *IEEE Photon. Technol. Lett.*, vol. 4, pp. 1103–1106, Oct. 1992.

[9] Y. Yamaguchi, A. Yamada, T. Otsubo, K. Shinone, K. Miyagi, and A. Taniguchi, "Tensile strained MQW semiconductor optical amplifier," in *Proc. 1995 IPRM 1995 Conf.*, 1995, pp. 500–503.

[10] T. Ito, N. Yoshimoto, K. Magari, and H. Sugiura, "Wide-band polarization-independent tensile-strained InGaAs MQW-SOA gate," *IEEE Photon. Technol. Lett.*, vol. 10, pp. 657–659, 1998.

[11] K. Magari, M. Okamoto, and Y. Noguchi, "1.55-(m polarization insensitive high-gain tensile-strained-barrier MQW optical amplifier," *IEEE Photon. Technol. Lett.*, vol. 3, pp. 998–1000, Nov. 1991.

[12] A. Godefroy, A. Le Corre, F. Clerot, S. Salaan, S. Loualiche, J. C. Simon, L. Henry, C. Vaudry, J. C. Keromnes, G. Joulie, and P. Lamouler, "1.55-μm polarization-insensitive optical amplifier with strain-balanced superlattice active layer," *IEEE Photon. Technol. Lett.*, vol. 7, p. 473, 1995.

[13] A. Mathur and P. Daniel Dapkus, "Polarization insensitive strained quantum well gain medium for lasers and optical amplifiers," *Appl. Phys. Lett.*, vol. 61, pp. 2845–2847, 1992.

[14] M. Joma, H. Horikawa, C. Q. Xu, K. Yamada, Y. Katoh, and T. Kamijoh, "Polarization insensitive semiconductor laser amplifier with tensile strained InGaAsP/InGaAsP multiple quantum well structure," *Appl. Phys. Lett*, vol. 62, pp. 121–122, 1993.

[15] L. F. Tiemeijer, P. J. A. Thijs, T. Van Dongen, R. W. M. Slootweg, J. M. M. van der Heijden, J. J. M. Binsma, and M. P. C. M. Krijn, "Polarization insensitive multiple quantum well laser amplifiers for the 1300 nm window," *App. Phys. Lett.*, vol. 62, pp. 826–828, 1993.

[16] D. Tishinin, K. Uppal, I. Kim, and P. Daniel Dapkus, "1.3-μm polarization insensitive amplifiers with integrated-mode transformers," *IEEE Photon. Technol. Lett.*, vol. 9, pp. 1337–1339, Oct. 1997.

[17] A. D. Carlo, A. Reale, L. Tocca, and P. Lugli, "Polarization-independent δ-strained semiconductor optical amplifiers: A tight-binding study," *IEEE J. Quantum Electron.*, vol. 34, pp. 1730–1739, 1998.

[18] M. Hovinen, B. Gopalan, F. G. Johnson, and M. Dagenais, "A novel structure of delta-strained quantum well for polarization insensitive semiconductor devices at 1.55 μm," in *Proc. IEEE Lasers and Electro-Optical Society Annu. Meeting*, Boston, MA, 1996.

[19] F. Seiferth, F. G. Johnson, S. A. Merritt, S. Fox, R. D. Whaley, Y. J. Chen, M. Dagenais, and D. R. Stone, "Polarization insensitive 1.55-μm optical amplifier with GaAs Delta-strained Ga0.47In0.53As quantum wells," *IEEE Photon. Technol. Lett.*, vol. 9, pp. 1340–1342, 1997.
[20] R. E. Bartolo, S. S. Saini, T. Ren, Y. Zhu, M. Dagenais, H. Shen, J. Pamulapati, W. Zhou, O. King, and F. G. Hohnson, "Plarization-independent waveguide mudulators using 1.57-μm δ-strained InGaAs–InGaAsP quantum wells," *IEEE Photon. Technol. Lett.*, vol. 11, pp. 554–556, 1999.
[21] C. G. V. de Walle, "Band lineups and deformation potentials in the model-solid thoery," *Phys. Rev. B*, vol. 39, p. 1871, 1989.
[22] J. C. Yi and N. Dagli, "Finite-element analysis of valence band structure and optical properties of quantum-wire arrays on vicinal substrates," *IEEE J. Quantum Electron.*, vol. 31, pp. 208–218, 1995.
[23] S. L. Chuang, *Physics of Optoelectronic Devices*. New York: Wiley, 1995.
[24] D. Ahn and S. L. Chuang, "Optical gain in a strained-layer quantum-well laser," *IEEE J. Quantum Electron.*, vol. 24, p. 2400, 1988.
[25] D. Ahn, "Theory of non-Markovian gain in strained-layer quantum-well lasers with many-body effects," *IEEE J. Quantum Electron.*, vol. 34, pp. 344–352, 1998.
[26] D. Ahn and S. L. Chuang, "The theory of strained-layer quantum-well lasers with bandgap renormalization," *IEEE J. Quantum Electron.*, vol. 30, pp. 350–365, 1994.
[27] J. Hades, B. Demeulenaere, R. Bates, D. Lenstra, T. D. Vosser, and H. Blok, "Difference between TE and TM modal gain in amplifying waveguides: Analysis and assessment of two perturbation approaches," *Opt. Quantum Electron.*, vol. 29, pp. 263–273, 1997.
[28] H. Ghafouri-Shiraz, *Fundamentals of Laser Diode Amplifiers*. New York: Wiley, 1996.

Yong-Sang Cho was born in Seoul, Korea, in 1973. He received the B.S. degree in electrical and electronic engineering from the University of Seoul, Seoul, Korea, in 1997, and the M.S. degree in electronic engineering from Yonsei University, Seoul, Korea, in 1999, where he is currently pursuing the Ph.D. degree in the Department of Electrical and Electronic Engineering.

During 1997–1999, he was a Research Assistant at the Photonics Research Center of the Korea Institute of Science and Technology, where he worked on semiconductor optical amplifiers. His research interests include broadband high-speed wavelength converters based on semiconductor optical amplifiers and multimode laser diodes.

Woo-Young Choi received the B.S., M.S., and Ph.D. degrees, all in electrical engineering and comupter science, from the Massachusetts Institute of Technology, Cambridge. For his Ph.D. dissertation, he investigated MBE-grown InGaAlAs laser diodes for fiber optic applications.

From 1994 to 1995, he was a post-doctoral Research Fellow at NTT Opto-electronics Labs, where he worked on femtosecond all-optical switching devices based low-temperature-grown InGaAlAs quantum wells. In 1995, he joined the Department of Electrical and Electronic Engineering, Yonsei University, Seoul, Korea, where he is presently an Associate Professor. His current research interests are in the area of high-speed information processing technology, including high-speed optoelectronics, high-speed electronic circuits, and microwave photonics